Power-Efficient Time-Domain Scheduling for ISAC Beamforming

Ebubekir Memisoglu, Muhammad Bilal Janjua, and Hüseyin Arslan, *Fellow, IEEE*

***Abstract*—Power efficiency is a critical metric for a sustainable 6G network. The emergence of integrated sensing and communication (ISAC) services leads to significant power consumption due to additional signal transmission for sensing. An ISAC beamforming is an efficient transmission method for reducing power consumption in mmWave multi-input multi-output (MIMO) systems while meeting the requirements of communication users (CUs) and sensing users (SUs). This approach is only feasible when both users are within the coverage of the same beam. Otherwise, separate beams are required which results in high power consumption. In this letter, we propose a novel time-domain scheduling method for ISAC beamforming to achieve high-power efficiency. The performance gains compared to conventional scheduling method are demonstrated for the different number of users, periodicity values, and user distribution ratios.**

***Index Terms*—Integrated sensing and communication (ISAC), mmWave, time-domain scheduling, beamforming, power efficiency.**

I. INTRODUCTION

IN THE forthcoming era of advanced wireless networks, the role of sensing is going to become more crucial than ever [1]. Within this context, a new concept integrated sensing and communication (ISAC) is introduced to provide sensing and communication services concurrently in 6G wireless networks. The emerging sensing services may require additional resource allocation along with the resources of communication services. The ISAC systems necessitate the utilization of the time, frequency, spatial, and power resources in an optimum way to meet both sensing and communication requirements. For ISAC in the mmWave systems, the power efficiency for the resource allocation becomes a key limiting factor in sustainable 6G systems [2].

There are two main approaches for the resource allocation of ISAC systems in the literature. The first approach shares the time-frequency resources in an optimum way to maximize the localization accuracy and communication data rate [3]. Specifically, a time-division ISAC scheme is proposed by providing good compatibility with the legacy communication systems [4]. Another study divides the time duration into two periods as ISAC period and pure communication period where channel estimation, user localization, and beamforming design are performed during ISAC period [5]. The second approach shares the spatial resources by an optimum beamforming design [6]. There are three different beamforming types for ISAC in the literature: communication beamforming, sensing beamforming, and ISAC beamforming [7]. The communication beamforming serves for communicating users (CUs), sensing beamforming serves for sensing users (SUs), and ISAC beamforming serves for both CUs and SUs. ISAC beamforming is only feasible if CU and SU are within the coverage of same beam. By using a single beam for both sensing and communication, ISAC beamforming enables the sharing of the same time-frequency resources in a power-efficient way. However, if CU and SU are within the coverage of different beams, the simultaneous signal transmission for sensing and communication by using the same time-frequency resources is achievable only by generating separate beams. For the shared resources between sensing and communication services, the same waveform or different waveforms can be deployed [8].

Many scheduling methods based on the various performance evaluation metrics, such as delay, throughput, fairness, and spectral efficiency have been developed in the literature for CUs [9]. However, a few scheduling methods have been developed recently for ISAC systems. For instance, in [10], the ISAC base station serves multiple users with non-orthogonal multiple access (NOMA) while performing target sensing using the superimposed communication signal. Here, the sensing targets are scheduled to increase the number of sensed targets within a time interval. The authors in [11] reuse the CU frequency resources at ISAC base station to serve the scheduled sensing targets with a different transmit beamforming. A joint beamforming and scheduling method in ISAC system for the ultra-reliable low latency communication (URLLC) requirements is proposed to optimize the performance tradeoff between the periodic and aperiodic traffics [12]. In this letter, the aperiodic traffic is initiated as a consequence of sensing specific events and competes against wireless channel resources with the periodic traffic. Up to now in the literature, the effects of time-frequency domain resource allocation on ISAC beamforming have not been investigated.

ISAC beamforming can efficiently meet the communication and sensing requirements for both CUs and SUs when they are within the coverage of same beam. However, when they are within the coverage of different beams, separate beamforming is necessary, and leads to power inefficiency. Conventionally, the resource allocation of CUs and SUs have not been considered to increase the probability of ISAC beamforming occurrence. In our proposed method, we introduce a time domain scheduling approach to enhance power efficiency in ISAC systems. This method increases the occurrence of

Manuscript received 31 July 2024; accepted 20 August 2024. Date of publication 23 August 2024; date of current version 9 October 2024. The work of Hüseyin Arslan was supported by the Scientific and Technological Research Council of Turkey (TUBITAK) under Grant 123E514. The associate editor coordinating the review of this article and approving it for publication was Y. C. Wu. *(Corresponding author: Ebubekir Memisoglu.)*

The authors are with the Department of Electrical and Electronics Engineering, Istanbul Medipol University, 34810 Istanbul, Türkiye (e-mail: ebubekir.memisoglu@std.medipol.edu.tr; muhammad.janjua@std.medipol.edu.tr; huseyinarslan@medipol.edu.tr).

Digital Object Identifier 10.1109/LWC.2024.3448528

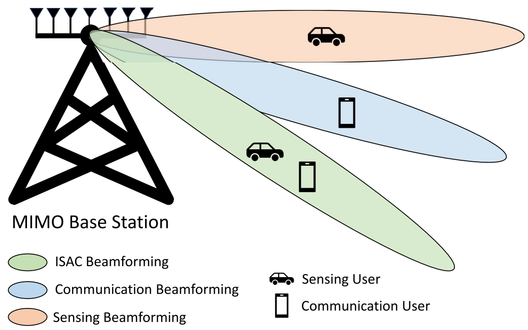

Fig. 1. The system model for the beamforming in ISAC systems.

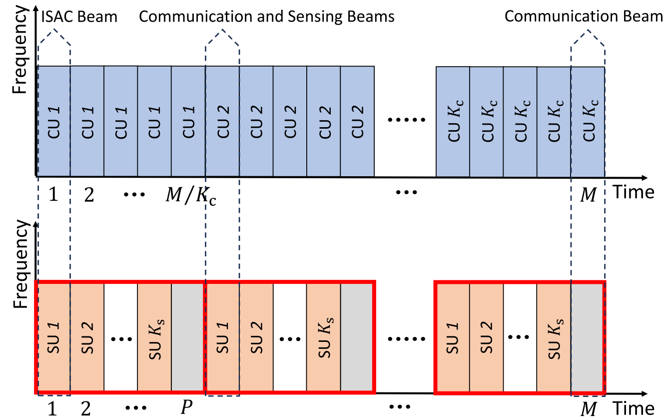

Fig. 2. The conventional scheduling for CUs and SUs over a frame.

ISAC beamforming by scheduling CUs based on the resource allocation of SUs in the time domain. As a result, the proposed scheduling method significantly improves power efficiency by reducing the number of beams generated per frame. We have evaluated the performance of this approach considering different numbers of users, periodicity values, and user distribution ratios.

II. System Model

Consider a mmWave massive multiple-input multiple-output (MIMO) base station that has a uniform linear array with N antennas to serve the single antenna $K_{\rm c}$ CUs and $K_{\rm s}$ SUs in downlink transmission as shown in Fig. 1. Although SU that receives the signal and performs sensing is considered, SU can be a passive target where it reflects the signal and the ISAC transceiver performs the sensing. For the beamforming, three types of beams are considered; communication, sensing, and ISAC beams. The communication, sensing, and ISAC signals within these beams are designed and used for serving CUs, SUs, and both CUs and SUs, respectively. Here, all beams are assumed to have the same beam pattern, ensuring equal power and beamwidth. The optimum design of the ISAC signal within the ISAC beam is studied in the literature [8]; however, it is assumed that the conventional communication signal within the ISAC beam is sufficient to meet the sensing requirements of SUs in this system model. The use of these beams is decided based on the spatial direction of CUs and SUs. It is assumed that the base station has two RF chains to serve simultaneously CU and SU. If CU and SU are within the coverage of same beam or a CU requests a data transmission, the base station only generates a single ISAC or communication beam, respectively. On the other hand, if CU and SU are within the coverage of different beams, the base station generates separate communication and sensing beams. Here, the total number of beams generated at the base station within a symbol duration is denoted by $K_{\rm b}$ where $K_{\rm b} \in \{1, 2\}$.

The conventional scheduling of the time resources for CUs and SUs is shown in Fig. 2. Here, the blue, orange, and gray rectangles represent the CU‘s, SU‘s and empty time resources, respectively. The channel accessing of multiple users can be orthogonally done in the time, frequency, and spatial domain; however, time and spatial domain channel accesses are considered in this system model. The base station allocates its resources over M time-domain symbols on a carrier. The $K_{\rm c}$ CUs share the total number of M symbols equally in the time domain with a time division multiple access scheme so that each CU has $M/K_{\rm c}$ symbols. The $K_{\rm s}$ SUs require a symbol within each subblock that has the size of P, where the total number of subblocks is denoted by R. Here, the periodicity of SUs is denoted by $\beta = 1/P$, and it is equal for all SUs. In Fig. 2, communication and sensing signals are transmitted differently for users in conventional systems. Specifically, communication signals are non-periodic, while sensing signals are periodic. As a result, the resource allocation for CUs consists of contiguous resources, while the resources for SUs consist of periodic resources over M symbols. The reason for the interleaved resources for SUs is to facilitate tracking for sensing functionalities. The base station utilizes different beam types based on the spatial direction of CUs and SUs. In a scenario where CU 1 and SU 1 share the same beam, and CU 2 and SU 1 have different beams, an ISAC beam is used for CU 1 and SU 1, while communication and sensing beams are used for CU 2 and SU 1. A communication beam is used when only CU requires signal transmission. By properly scheduling CUs and SUs, the number of generated beams in the system can be reduced, as depicted in Fig. 2.

At the MIMO base station, the signal vector $\boldsymbol{s}_m$ for the m-th symbol with normalized power $\mathbb{E}(\boldsymbol{s}_m \boldsymbol{s}_m^H) = \mathbf{I}_{K_{\rm b}}$ is modulated as

$$\boldsymbol{s}_m = \begin{cases} [s_{\rm c}]^T, & K_{\rm b} = 1 \\ [s_{\rm c} \;\; s_{\rm s}]^T, & K_{\rm b} = 2, \end{cases} \tag{1}$$

where $s_{\rm c}$, $s_{\rm s}$, and $\mathbf{I}_{K_{\rm b}}$ represent the communication data symbol, sensing symbol, and the identity matrix of size $K_{\rm b}$, respectively. Here, the transposition and Hermitian transposition are denoted by $(.)^T$ and $(.)^H$, respectively. After obtaining $\boldsymbol{s}_m$, each beam is generated with a constant transmit power ρ.

For the beamspace MIMO, the spatial discrete Fourier transform matrix $\mathbf{U} \in \mathbb{C}^{N \times N}$ has the array steering vectors of N orthogonal directions as

$$\mathbf{U} = \left[\mathbf{u}(\bar{\phi}_1) \; \mathbf{u}(\bar{\phi}_2) \; \ldots \; \mathbf{u}(\bar{\phi}_N)\right]^H, \tag{2}$$

where $\mathbf{u}(\bar{\phi}_n) \in \mathbb{C}^{N\times 1}$ is the array steering vector with the predefined spatial direction $\bar{\phi}_n = \frac{1}{N}(n - \frac{N+1}{2})$ for $n = 1, 2, \ldots N$. For a uniform linear array with N antennas, $\mathbf{u}(\bar{\phi}_n)$ is defined as

$$\mathbf{u}(\bar{\phi}_n) = \frac{1}{\sqrt{N}}\left[e^{-j2\pi\theta\nu}\right]_{\nu\in\Upsilon(N)}, \tag{3}$$

$$\Upsilon(N) = (q - (N-1)/2,\ \ q = 0, 1, \ldots, N-1), \tag{4}$$

where $\bar{\phi}_n = \frac{d}{\lambda}\sin\theta$ represent the spatial direction with the parameters of the physical direction θ, signal wavelength λ, and antenna spacing $d = \lambda/2$.

For the wireless channel between the transmitter and receiver, the Saleh-Valenzuela channel model for mmWave systems [13] is used to obtain the channel vector $\mathbf{h}_{k_c,m}$ for the *m*-th symbol of the k_c-th CU as

$$\mathbf{h}_{k_c,m} = \alpha^{(0)}_{k_c,m}\mathbf{u}\left(\phi^{(0)}_{k_c,m}\right) + \sum_{l=1}^{L}\alpha^{(l)}_{k_c,m}\mathbf{u}\left(\phi^{(l)}_{k_c,m}\right), \tag{5}$$

where $\alpha^{(0)}_{k_c,m}$ and $\alpha^{(l)}_{k_c,m}$, and $\phi^{(0)}_{k_c,m}$ and $\phi^{(l)}_{k_c,m}$ represent the complex channel gains, and the path angles for the line-of sight $(l = 0)$ and non-line-of-sight $(1 \le l \le L)$ paths, respectively. The channel vector $\mathbf{h}_{k_s,m}$ for the *m*-th symbol of the k_s-th SU is also obtained as in (5). Here, the non-line-of-sight paths are not considered so that $\alpha^{(l)}_{k_c,m} = 0$ and $\alpha^{(l)}_{k_s,m} = 0$ for $l = 1, 2, \ldots, L$.

For the *m*-th symbol, if a single beam $(K_b = 1)$ is deployed, the received signal vector for CU $(\mathbf{y}_{c_m})$ and SU$(\mathbf{y}_{s_m})$ is taken as

$$\begin{aligned}\mathbf{y}_{c_m} &= \mathbf{h}^H_{k_c,m}\mathbf{U}^H\mathbf{G}\mathbf{s}_m + \mathbf{n}_m,\\ \mathbf{y}_{s_m} &= \mathbf{h}^H_{k_s,m}\mathbf{U}^H\mathbf{G}\mathbf{s}_m + \mathbf{n}_m,\end{aligned} \tag{6}$$

where $\mathbf{n}_m \in \mathbb{C}^{K_b\times 1}$ is the additive white Gaussian noise with the distribution of $\mathcal{CN}(0, \sigma^2\mathbf{I}_{K_b})$ for the *m*-th symbol. Here, $\mathbf{G}$ is the zero-forcing precoding matrix with the size of $N \times K_b$. If multiple beams $(K_b = 2)$ are deployed, the received signal vectors $\mathbf{y}_{c_m}$ and $\mathbf{y}_{s_m}$ are obtained as

$$[\mathbf{y}_{c_m}\ \mathbf{y}_{s_m}] = \left[\mathbf{h}_{k_c,m}\ \mathbf{h}_{k_s,m}\right]^H\mathbf{U}^H\mathbf{G}\mathbf{s}_m + \mathbf{n}_m. \tag{7}$$

Also, the channels of CUs and SUs are assumed as constant over the *M* symbols.

III. Proposed Scheduling Method

Conventionally, a mmWave MIMO base station can generate multiple beams simultaneously, where $K_b > 2$. These beams cover all CUs and SUs in the environment. In this case, the proposed method is applied to the selected two beams, where K_c CUs and K_s SUs exist on these beams. Also, the proposed method can be independently applied to another two beams in the system. Therefore, the proposed method is directly applicable to the scenarios of $K_b > 2$.

In the considered system model, the base station generates two beams simultaneously with the spatial directions $\phi^{(0)}_{k_c,m}$, $\phi^{(0)}_{k_s,m} \in \{\bar{\phi}_{n_1}, \bar{\phi}_{n_2}\}$ where $n_1 \ne n_2$. Therefore, the K_c CUs and K_s SUs are located within the coverage of these beams, where $K_c \ge 2$ and $K_s \ge 2$. The first group of CUs and SUs is within the coverage of the same beam but has a different beam from the other group. To group the users, the first $\varphi_c K_c$ CUs and $\varphi_s K_s$ SUs are located on the beam with the spatial direction $\bar{\phi}_{n_1}$, then the rest $(K_c - \varphi_c K_c)$ CUs and $(K_s - \varphi_s K_s)$ SUs are located on the beam with the spatial direction $\bar{\phi}_{n_2}$. The parameters φ_c and φ_s are used to change the distribution of CUs and SUs on the beams, where $0 < \varphi_c < 1$ and $0 < \varphi_s < 1$, and $\varphi_c K_c$ and $\varphi_s K_s$ are positive integer values. The beam index vector of the CUs is obtained as

$$\Phi_c(k_c) = \begin{cases}\bar{\phi}_{n_1},\ k_c \le \varphi_c K_c\\ \bar{\phi}_{n_2},\ k_c > \varphi_c K_c\end{cases} \tag{8}$$

for $k_c = 1, 2, \ldots, K_c$. The beam index vector of the SUs $\mathbf{\Phi}_s \in \mathbb{Z}^{K_s\times 1}$ is obtained similarly in (8) as

$$\Phi_s(k_s) = \begin{cases}\bar{\phi}_{n_1},\ k_s \le \varphi_s K_s\\ \bar{\phi}_{n_2},\ k_s > \varphi_s K_s\end{cases} \tag{9}$$

for $k_s = 1, 2, \ldots, K_s$.

The time resources on a frame are allocated for the CUs and SUs for the conventional scheduling method as shown in Fig. 2. The resource allocation vectors of conventional scheduling for CUs and SU are represented as

$$\Omega_c(m) = \begin{cases}k_c,\ (k_c - 1)(M/K_c) + 1 \le m \le k_c(M/K_c)\\ 0,\ \ \text{otherwise}\end{cases} \tag{10}$$

and

$$\Omega_s(m) = \begin{cases}k_s,\ \mathrm{mod}(m-1, P)\ + 1 = k_s\\ 0,\ \ \text{otherwise}\end{cases} \tag{11}$$

for $m = 1, 2, \ldots, M$ and mod(*a*, *b*) calculates the remainder after dividing *a* by *b*. According to their resource allocation vectors $\mathbf{\Omega}_c$ and $\mathbf{\Omega}_s$, the spatial direction vectors of each symbol on the frame for CUs and SUs are obtained as

$$\Psi_c(m) = \begin{cases}\bar{\phi}_{n_1},\ 1 \le m \le \varphi_c M\\ \bar{\phi}_{n_2},\ \varphi_c M + 1 \le m \le M\end{cases} \tag{12}$$

and

$$\Psi_s(m) = \begin{cases}\bar{\phi}_{n_1},\ \mathrm{mod}(m-1, P)\ + 1 \le \varphi_s K_s\\ \bar{\phi}_{n_2},\ \varphi_s K_s + 1 \le \mathrm{mod}(m-1, P)\ + 1 \le K_s\\ 0,\ \ \ \text{otherwise.}\end{cases} \tag{13}$$

To apply the proposed scheduling method, firstly, the indices of $\bar{\phi}_{n_1}$ and $\bar{\phi}_{n_2}$ in the $\mathbf{\Psi}_c$ and $\mathbf{\Psi}_s$ are determined. The indices of CUs and SUs with first and second spatial direction are denoted as $\mathbf{\Lambda}_{c_1}$, $\mathbf{\Lambda}_{c_2}$, $\mathbf{\Lambda}_{s_1}$, and $\mathbf{\Lambda}_{s_2}$, respectively. These index vectors represent the symbol indices of CUs and SUs that have the spatial directions $\bar{\phi}_{n_1}$ and $\bar{\phi}_{n_2}$ as

$$\mathbf{\Lambda}_{c_1} = [1, 2, \ldots, \varphi_c M]^T, \tag{14}$$

$$\mathbf{\Lambda}_{c_2} = [\varphi_c M + 1, \varphi_c M + 2, \ldots, M]^T, \tag{15}$$

$$\begin{aligned}\mathbf{\Lambda}_{s_1} = [&1, 2, \ldots, \varphi_s K_s, P+1, P+2, \ldots, P + \varphi_s K_s, \ldots,\\ &(R-1)P + 1, (R-1)P + 2, \ldots, (R-1)P + \varphi_s K_s]^T,\end{aligned} \tag{16}$$

$$\begin{aligned}\mathbf{\Lambda}_{s_2} = [&\varphi_s K_s + 1, \varphi_s K_s + 2, \ldots, K_s, P + \varphi_s K_s + 1,\\ &P + \varphi_s K_s + 2, \ldots, P + K_s, \ldots, (R-1)P + \varphi_s K_s + 1,\\ &(R-1)P + \varphi_s K_s + 2, \ldots, (R-1)P + K_s]^T,\end{aligned} \tag{17}$$

where $M = R \cdot P$. Here, the proposed method only schedules the K_c CUs based on the obtained vectors in (14)-(17). Initially, the conventional scheduling is applied as $\mathbf{\Omega}^p_c = \mathbf{\Omega}_c$.

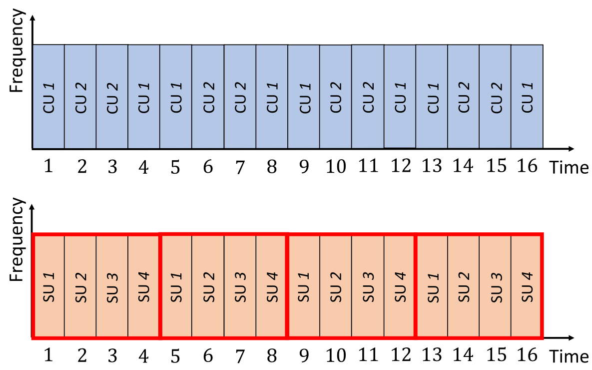

Fig. 3. The proposed scheduling method for a simple scenario.

Then, the resources of CUs for the proposed method are scheduled as

$$\Omega_{\mathrm{c}}^{\mathrm{p}}(\Lambda_{\mathrm{s}_1}(i_{\mathrm{s}_1}) = \Omega_{\mathrm{c}}(\Lambda_{\mathrm{c}_1}(i_{\mathrm{c}_1})), \quad \forall\ i_{\mathrm{s}_1} = i_{\mathrm{c}_1}, \tag{18}$$

$$\Omega_{\mathrm{c}}^{\mathrm{p}}(\Lambda_{\mathrm{s}_2}(i_{\mathrm{s}_2})) = \Omega_{\mathrm{c}}(\Lambda_{\mathrm{c}_2}(i_{\mathrm{c}_2})), \quad \forall\ i_{\mathrm{s}_2} = i_{\mathrm{c}_2}, \tag{19}$$

where $i_{\mathrm{c}_1} \in \{1, 2, \ldots, \varphi_{\mathrm{c}} M\}$, $i_{\mathrm{c}_2} \in \{1, 2, \ldots, (M - \varphi_{\mathrm{c}} M)\}$, $i_{\mathrm{s}_1} \in \{1, 2, \ldots, \varphi_{\mathrm{s}} K_{\mathrm{s}} R\}$, and $i_{\mathrm{s}_2} \in \{1, 2, \ldots, (K_{\mathrm{s}} - \varphi_{\mathrm{s}} K_{\mathrm{s}}) R\}$. As deduced from (10), (14), and (15), different K_{c} values do not change the proposed scheduling in (18). After the proposed scheduling of the CUs based on the conventional scheduling of SUs, the number of beams that need to be generated at the base station decreases.

To illustrate the proposed method, a simple scenario with the parameters of $M = 16$, $K_{\mathrm{c}} = 2$, $K_{\mathrm{s}} = 4$, $\beta = 1/4$, $\varphi_{\mathrm{c}} = \varphi_{\mathrm{s}} = 1/2$, $\Phi_{\mathrm{c}}(k_{\mathrm{c}} = 1) = \Phi_{\mathrm{s}}(k_{\mathrm{s}} = 1, 4)$, $\Phi_{\mathrm{c}}(k_{\mathrm{c}} = 2) = \Phi_{\mathrm{s}}(k_{\mathrm{s}} = 2, 3)$, and $\Phi_{\mathrm{c}}(k_{\mathrm{c}} = 1) \neq \Phi_{\mathrm{s}}(k_{\mathrm{s}} = 2, 3)$ is provided in Fig. 3. Since the spatial direction of the users on each symbol time is the same, the proposed method uses only ISAC beamforming for the frame shown in Fig. 3. On the other hand, if conventional scheduling is applied for this scenario, separate communication and sensing beamforming are required. Note that the proposed method only schedules the resources of CUs compared to conventional scheduling to improve the power efficiency.

Since the orthogonal steering vectors are used and the line-of-sight channel is considered, the beams on the spatial directions $\bar{\phi}_{n_1}$ and $\bar{\phi}_{n_2}$ do not interfere with each other. Then, the signal-to-noise ratio (SNR) for the CU and SU symbol on the m-th symbol is obtained as

$$\gamma_{\mathrm{c}_m} = \frac{\rho}{\sigma^2 \left(\mathbf{h}_{k_{\mathrm{c}},m}^H \mathbf{h}_{k_{\mathrm{c}},m}\right)^{-1}}, \quad \gamma_{\mathrm{s}_m} = \frac{\rho}{\sigma^2 \left(\mathbf{h}_{k_{\mathrm{s}},m}^H \mathbf{h}_{k_{\mathrm{s}},m}\right)^{-1}}. \tag{20}$$

As deduced from (20), the proposed method does not affect the received SNR values for CU and SU. According to γ_{c_m}, the capacity of CUs on the m-th symbol can be calculated as

$$\mathrm{C}_m = log_2(1 + \gamma_{\mathrm{c}_m}). \tag{21}$$

Lastly, the average transmit power efficiency is defined as [14],

$$\varepsilon_P = \frac{1}{M} \sum_{m=1}^{M} \frac{\mathrm{C}_m}{K_{\mathrm{b}_m}(\rho + P_{RF})}, \tag{22}$$

where K_{b_m} is the number of used beams for the m-th symbol and P_{RF} is the power consumed in the components per RF chain. The proposed method changes the value of K_{b_m} for the m-th symbol to improve ε_P compared to conventional scheduling.

For the complexity, the proposed scheduling and beamforming processes are considered. The proposed method only requires performing the assignment operations in (18) and (19) in addition to the digital signal processes at a conventional mmWave MIMO transmitter. The total number of beams generated over the frame has a proportional relationship with the beamforming complexity [13], where the total number of beams are calculated as $\sum_{m=1}^{M} K_{\mathrm{b}_m}$. Since the proposed method decreases the total number of beams in ISAC system, it has a lower beamforming complexity than conventional method.

IV. Simulation Results

In this section, computer simulations are performed to evaluate the power efficiency of the proposed method compared to the conventional method in mmWave MIMO systems. The performance is investigated for the different parameters of the number of users $(K_{\mathrm{c}}, K_{\mathrm{s}})$, periodicity (β), and user distribution ratios $(\varphi_{\mathrm{c}}, \varphi_{\mathrm{s}})$. The base station is equipped with the uniform linear array (ULA) with $N = 256$ and $K_{\mathrm{b}} = 2$RF chains. The consumed power in each RF is taken as $P_{RF} = 34.4mW$ [14]. The spatial directions of the beams are assumed as $\bar{\phi}_{64}$ and $\bar{\phi}_{193}$, and $\phi_{k_{\mathrm{c}},m}^{(0)}, \phi_{k_{\mathrm{s}},m}^{(0)} \in \{\bar{\phi}_{64}, \bar{\phi}_{193}\}$. The channel gain of the line-of-sight path has a distribution as $\alpha_{k_{\mathrm{c}},m}^{(0)}, \alpha_{k_{\mathrm{s}},m}^{(0)} \sim \mathcal{CN}(0, 1)$. One frame consists of $M = 64$ symbols and the frame is generated 10^4 times for Monte Carlo simulations. For the scheduling of CUs, (10) are used for the conventional method, while (18) and (19) are employed for the proposed method.

Fig. 4(a) shows the power efficiency (ε_P) performance of the proposed method with different K_{c} and K_{s} values for $\beta = 1/8$ and $\varphi_{\mathrm{c}} = \varphi_{\mathrm{s}} = 4/8$. The power efficiency of the conventional scheduling method decreases when the number of SUs increases. If there is no SU in the system, the power efficiency is optimum. However, the base station requires to generate more sensing beams with the increase of the number of SUs due to conventional scheduling. Then, this causes a decrease in power efficiency. On the other hand, the proposed scheduling method obtains a better power efficiency than conventional scheduling due to scheduling the CU according to the resource allocation of SUs. Thus, the proposed method achieves the better power efficiency for different numbers of users. The reason for the same performance in all cases is that an additional sensing beam is not required due to the proposed scheduling in the considered scenario. Also, the power efficiency performance does not change for different K_{c} values in both conventional and proposed methods. Because the symbol index vectors of the spatial directions in (14) and (15) remain constant regardless of the number of CUs.

Fig. 4(b) shows the ε_P performance of the proposed method with different periodicity values of SUs for $K_{\mathrm{c}} = K_{\mathrm{s}} = 2$ and $\varphi_{\mathrm{c}} = \varphi_{\mathrm{s}} = 4/8$. If β increases, the power efficiency

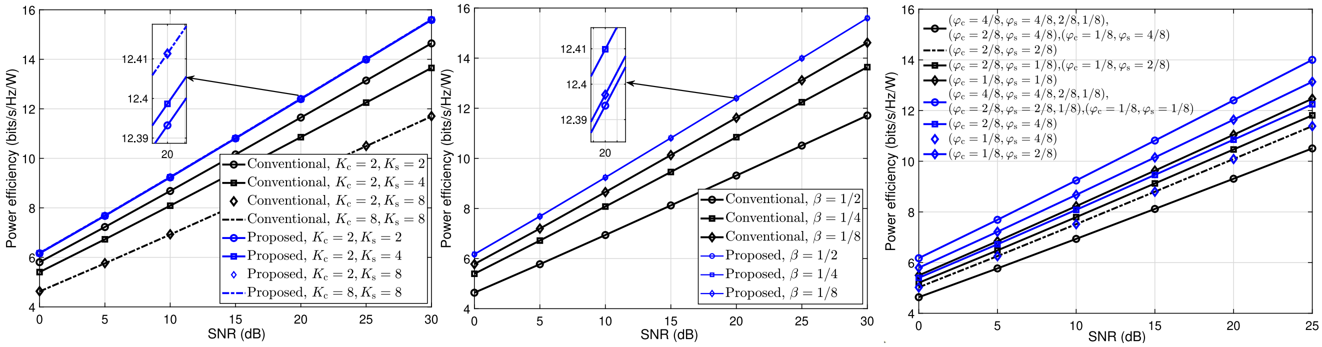

(a) (b) (c)

Fig. 4. Power efficiency performance results of the proposed method for the different number of users (a), periodicity values (b), and user distribution ratios (c).

decreases for the conventional scheduling method. When the β is increased, the requirement of signal transmission for SUs will be higher. Therefore, the power efficiency will be better for lower β values in the conventional method. On the other hand, the proposed method achieves the best performance even if the β increases. For instance, the proposed method can improve the power efficiency by approximately 33.3% for $\beta = 1/2$.

Fig. 4(c) shows the ε_P performance of the proposed method with different user distribution ratios for $K_c = K_s = 8$ and $\beta = 1/8$. In the figure, the black and blue plots depict the results of conventional and proposed methods for different values of (φ_c, φ_s), respectively. The better power efficiency performance gain is achieved for the proposed method when there is equal user distribution on the beams. While φ_c is fixed, a decrease in φ_s leads to a reduction in the performance gain of the proposed method. Similarly, while φ_s is fixed, decreasing φ_c results in a decreased performance gain for the proposed method. However, in some cases, reducing the values of φ_c and φ_s does not alter the performance gain. Accordingly, as the distribution ratios approach to 0, the power efficiency performance of conventional method tends to increase. As shown in the figure, the proposed method does not achieve the best efficiency for the cases of $(\varphi_c = 2/8, \varphi_s = 4/8)$, $(\varphi_c = 1/8, \varphi_s = 4/8)$, and $(\varphi_c = 1/8, \varphi_s = 2/8)$, but it always outperforms the conventional method. Additionally, the performance gains of the proposed method for all scenarios in Fig. 4 improve at higher SNR values.

V. Conclusion

A novel time-domain scheduling of CUs according to the resource allocation of SUs has been proposed to increase the occurrence of ISAC beamforming in mmWave MIMO systems. The simulation results demonstrate that the proposed method achieves a significant power efficiency improvement compared to conventional resource allocation. Especially, the performance gain is higher for a high number of users, high periodicity values, and equal user distribution because the occurrence of ISAC beamforming is lower for conventional scheduling in these conditions. For future work, the scheduling methods developed for communication services will be combined and integrated with the proposed scheduling method in ISAC systems.

References

[1] F. Liu et al., "Integrated sensing and communications: Toward dual-functional wireless networks for 6G and beyond," *IEEE J. Sel. Areas Commun.*, vol. 40, no. 6, pp. 1728–1767, Jun. 2022.

[2] W. Wu et al., "Revisiting the system energy footprint and power efficiency on the way to sustainable 6G systems," *IEEE Wireless Commun.*, vol. 29, no. 6, pp. 6–8, Dec. 2022.

[3] B. Li et al., "Value of service maximization in integrated localization and communication system through joint resource allocation," *IEEE Trans. Commun.*, vol. 71, no. 8, pp. 4957–4971, Aug. 2023.

[4] H. Zhang et al., "Time allocation approaches for a perceptive mobile network using integration of sensing and communication," *IEEE Trans. Wireless Commun.*, vol. 23, no. 2, pp. 1158–1169, Feb. 2024.

[5] X. Hu, C. Liu, M. Peng, and C. Zhong, "IRS-based integrated location sensing and communication for mmWave SIMO systems," *IEEE Trans. Wireless Commun.*, vol. 22, no. 6, pp. 4132–4145, Jun. 2023.

[6] H. Hua, J. Xu, and T. X. Han, "Optimal transmit beamforming for integrated sensing and communication," *IEEE Trans. Veh. Technol.*, vol. 72, no. 8, pp. 10588–10603, Aug. 2023.

[7] F. Dong et al., "Sensing as a service in 6G perceptive networks: A unified framework for ISAC resource allocation," *IEEE Trans. Wireless Commun.*, vol. 22, no. 5, pp. 3522–3536, May 2023.

[8] E. Memisoglu et al., "Waveform design with constellation extension for OFDM dual-functional radar-communications," *IEEE Trans. Veh. Technol.*, vol. 72, no. 11, pp. 14245–14254, Nov. 2023.

[9] A. Mamane et al., "Scheduling algorithms for 5G networks and beyond: Classification and survey," *IEEE Access*, vol. 10, pp. 51643–51661, 2022.

[10] C. Dou, N. Huang, Y. Wu, L. Qian, and T. Q. Quek, "Sensing-efficient NOMA-aided integrated sensing and communication: A joint sensing scheduling and beamforming optimization," *IEEE Trans. Veh. Technol.*, vol. 72, no. 10, pp. 13591–13603, Oct. 2023.

[11] C. Dou, N. Huang, Y. Wu, L. Qian, and T. Q. Quek, "Channel sharing aided integrated sensing and communication: An energy-efficient sensing scheduling approach," *IEEE Trans. Wireless Commun.*, vol. 23, no. 5, pp. 4802–4814, May 2024, doi: 10.1109/TWC.2023.3322680.

[12] X. Zhao and Y.-J. A. Zhang, "Joint beamforming and scheduling for integrated sensing and communication systems in URLLC," in *Proc. IEEE Glob. Commun. Conf. (GLOBECOM)*, 2022, pp. 1–6.

[13] J. Brady, N. Behdad, and A. M. Sayeed, "Beamspace MIMO for millimeter-wave communications: System architecture, modeling, analysis, and measurements," *IEEE Trans. Antennas Propag.*, vol. 61, no. 7, pp. 3814–3827, Jul. 2013.

[14] P. V. Amadori and C. Masouros, "Low RF-complexity millimeter-wave beamspace-MIMO systems by beam selection," *IEEE Trans. Commun.*, vol. 63, no. 6, pp. 2212–2223, Jun. 2015.